

Temperature-dependent phase noise properties of a two-section GaSb-based mode-locked laser emitting at $2\ \mu\text{m}$

Cite as: Appl. Phys. Lett. **117**, 141103 (2020); <https://doi.org/10.1063/5.0024064>

Submitted: 04 August 2020 . Accepted: 23 September 2020 . Published Online: 05 October 2020

Xiang Li,  Hong Wang,  Zhongliang Qiao, Jia Xu Brian Sia, Wanjun Wang, Xin Guo, Yu Zhang, Zhichuan Niu, Cunzhu Tong, and Chongyang Liu



View Online



Export Citation



CrossMark

ARTICLES YOU MAY BE INTERESTED IN

[Trapping of multiple H atoms at the Ga\(1\) vacancy in \$\beta\text{-Ga}_2\text{O}_3\$](#)

Applied Physics Letters **117**, 142101 (2020); <https://doi.org/10.1063/5.0024269>

[Thermoelectric \$\text{Si}_{1-x}\text{Ge}_x\$ and Ge epitaxial films on Si\(001\) with controlled composition and strain for group IV element-based thermoelectric generators](#)

Applied Physics Letters **117**, 141602 (2020); <https://doi.org/10.1063/5.0023820>

[Low temperature homoepitaxy of \(010\) \$\beta\text{-Ga}_2\text{O}_3\$ by metalorganic vapor phase epitaxy: Expanding the growth window](#)

Applied Physics Letters **117**, 142102 (2020); <https://doi.org/10.1063/5.0023778>

HIDEN
ANALYTICAL

Instruments for **Advanced Science**

- Knowledge,
- Experience,
- Expertise

[Click to view our product catalogue](#)

Contact Hiden Analytical for further details:

www.HidenAnalytical.com
info@hiden.co.uk



Gas Analysis

- ▶ dynamic measurement of reaction gas streams
- ▶ catalysis and thermal analysis
- ▶ molecular beam studies
- ▶ dissolved species probes
- ▶ fermentation, environmental and ecological studies



Surface Science

- ▶ UHVTPD
- ▶ SIMS
- ▶ end point detection in ion beam etch
- ▶ elemental imaging - surface mapping



Plasma Diagnostics

- ▶ plasma source characterization
- ▶ etch and deposition process reaction kinetic studies
- ▶ analysis of neutral and radical species



Vacuum Analysis

- ▶ partial pressure measurement and control of process gases
- ▶ reactive sputter process control
- ▶ vacuum diagnostics
- ▶ vacuum coating process monitoring

Temperature-dependent phase noise properties of a two-section GaSb-based mode-locked laser emitting at 2 μm

Cite as: Appl. Phys. Lett. **117**, 141103 (2020); doi: [10.1063/5.0024064](https://doi.org/10.1063/5.0024064)

Submitted: 4 August 2020 · Accepted: 23 September 2020 ·

Published Online: 5 October 2020



View Online



Export Citation



CrossMark

Xiang Li,¹ Hong Wang,^{2,a)}  Zhongliang Qiao,³  Jia Xu Brian Sia,² Wanjun Wang,² Xin Guo,² Yu Zhang,⁴ Zhichuan Niu,^{4,a)} Cunzhu Tong,⁵ and Chongyang Liu^{1,a)}

AFFILIATIONS

¹Temasek Laboratories, Nanyang Technological University, 50 Nanyang Drive, Singapore 637553, Singapore

²School of Electrical and Electronic Engineering, Nanyang Technological University, 50 Nanyang Avenue, Singapore 639798, Singapore

³Key Laboratory of Laser Technology and Optoelectronic Functional Materials of Hainan Province, and School of Physics and Electronic Engineering, Hainan Normal University, No. 99 Longkun Road, Haikou 571158, China

⁴State Key Lab for Superlattices and Microstructures, Institute of Semiconductors, Chinese Academy of Sciences, No.A35 QingHua East Road, Beijing 100083, China, and College of Materials Science and Opto-Electronic Technology, University of Chinese Academy of Sciences, No.380 Huaibei, Beijing 101408, China

⁵State Key Lab of Luminescence and Applications, Changchun Institute of Optics, Fine Mechanics and Physics, Chinese Academy of Sciences, No.3888 Dong Nanhu Road, Changchun 130033, China

^{a)}Authors to whom correspondence should be addressed: ewanghong@ntu.edu.sg; zcniu@semi.ac.cn; and liucy@ntu.edu.sg

ABSTRACT

The temperature-dependent phase noise properties of a monolithic two-section mode-locked semiconductor laser are first investigated. This is performed on a GaSb-based quantum well laser emitting at $\sim 2 \mu\text{m}$. Stable mode locking operation with a fundamental repetition frequency of $\sim 13.3 \text{ GHz}$ is achieved on this laser up to 60°C . At a fixed temperature, there is no monotonous dependence of integrated jitter on the bias condition. For a given gain current or absorber voltage, there exists a corresponding optimal absorber voltage or gain current, respectively, that minimizes the integrated jitter. More important, the phase noise properties improve obviously at elevated temperatures with the lowest achievable jitter reducing obviously from 3.15 ps at 20°C to 1.39 ps at 60°C (100 kHz – 1 GHz). We consider that the reason is reduced amplified spontaneous emission noise at high temperatures. This is confirmed by the extracted peak-to-valley ratio of the involved laser modes. We believe that this study provides an important insight into the carrier behaviors and noise performance of mode-locked semiconductor lasers, which is meaningful to their applications especially at high temperatures.

Published under license by AIP Publishing. <https://doi.org/10.1063/5.0024064>

Monolithic mode-locked semiconductor lasers, taking advantage of their compactness, easy electrical pump, integration feasibility with silicon photonic circuits, and capability of easily generating pulse trains at multi gigahertz repetition rates, have attracted increasing attention in high-capacity optical communications, high-density optical storage, optical clocking for electronic circuits, light detection and ranging (LIDAR), seed light generation, etc.^{1–7}

The phase noise (PN) properties of such mode-locked lasers (MLLs) are important parameters that are directly related to the time resolution, bit error rate, or data transmitting capacity when they are used for the above applications. Therefore, a thorough phase noise

study is necessary to find out their optimal configuration and working conditions as well as some guidelines for improving their noise performance. There are several papers reporting on this topic. For example, Thompson *et al.* investigated the influences of the gain-to-absorber length ratio on the timing jitter performance on $1.3 \mu\text{m}$ GaAs-based passively mode-locked quantum dot lasers. The finding is a shorter absorber which is preferred to obtain lower timing jitter.⁸ Todaro *et al.* also carried out a systematic bias-dependent timing jitter study on $1.3 \mu\text{m}$ GaAs-based passively mode-locked quantum dot lasers, which points out that for a given absorber voltage, there exists an optimal gain current that minimizes timing jitter.⁹ In addition, the

bias-dependent radio frequency (RF) linewidths of 1.3 and 1.55 μm mode-locked semiconductor lasers have also been reported.^{10,11} However, the temperature dependence of the phase noise performance of such MLLs, especially GaSb-based ones at longer wavelengths has never been reported and remains unclear, while elevated temperature is inevitable in many practical applications. It is important to investigate it to meet the requirements for these related applications.

To investigate this issue, a two-section GaSb-based passively MLL emitting at 2 μm is presented in this work. The 2 μm wavelength band is promising for numerous applications in communication, sensing, medicine, and military.^{12–15} Stable mode locking up to 60 $^{\circ}\text{C}$ is achieved on this laser. The bias- and temperature-dependent phase noise properties of the laser are systematically investigated.

The epi-wafer used for device fabrication was grown on a (100) n-GaSb substrate by molecular beam epitaxy (MBE). Its active region consists of a single compressively strained ($\sim 1.26\%$) $\text{In}_{0.2}\text{Ga}_{0.8}\text{Sb}$ quantum well. The detailed laser structure and fabrication process can be found in our previous work.¹⁶ The laser under test in this study has a total cavity length of ~ 2.94 mm and its ridge width is ~ 5 μm which provides single lateral mode operation. The total cavity length includes a gain section ($L_g \sim 2.63$ mm), an absorber section ($L_a \sim 0.30$ mm), and a 10 μm -wide electrical isolation area between the two sections. Both facets are as-cleaved. When working in the stable mode locking regime, the gain section is forward biased (I_g), while the absorber section needs to be reverse biased (V_a). During the tests, the two-section laser was placed with the p-side up on a laser testing stage equipped with a temperature electronic controller (TEC).

Figure 1 shows the temperature-dependent average light output power vs injection current (I - I) curves of the tested laser under DC bias when the absorber is unconnected ($V_a = 0$ V). The output power was collected from the facet of the gain section. The operation temperature is raised to 80 $^{\circ}\text{C}$ which is limited by the TEC. As the temperature rises, the turn-on jump becomes more and more distinct, and the hysteresis loop starts to emerge at 60 $^{\circ}\text{C}$. This bistability phenomenon has been observed in some studies,^{17,18} while others did not observe it.⁴ The origin of it was proved to be related to the intensity-dependent absorption of the saturable absorber.^{17,19}

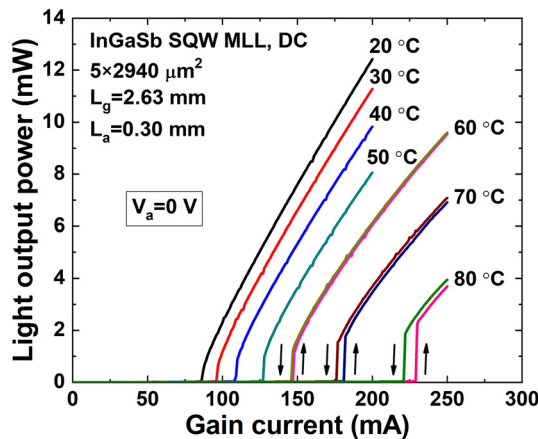


FIG. 1. Temperature-dependent L-I curves with the absorber unconnected ($V_a = 0$ V) from the tested two-section MLL. The hysteresis loop starts to emerge at 60 $^{\circ}\text{C}$.

Stable mode locking was achieved over a wide range of bias conditions on the tested two-section MLL. Figure 2(a) shows a typical RF spectrum at 20 $^{\circ}\text{C}$ ($I_g = 190$ mA, $V_a = -1.6$ V). It was measured using a high-speed photo detector (EOT ET-5000F) followed by a 50 GHz RF spectrum analyzer (Agilent N9030A). The fundamental repetition frequency is at ~ 13.3 GHz featured by a very strong RF signal with more than 70 dB signal to noise ratio. This fundamental repetition frequency is determined by the photon round trip time in the 2.94 mm-long laser cavity. The inset in Fig. 2(a) shows the corresponding optical spectrum under this bias condition. This spectrum can be well fitted to a Gaussian curve ($r^2 = 0.998$). The spectrum centering at ~ 1958 nm (~ 153.2 THz) has a full width at half maximum (FWHM) of ~ 5.9 nm (~ 464 GHz), and more than 60 longitudinal modes spaced by ~ 0.17 nm (~ 13.3 GHz) are included. If unchirped Gaussian pulses which have a time-bandwidth product of ~ 0.441 are assumed, a minimum pulse width of ~ 1 ps can be expected. Using the pulse width estimation method in Ref. 4 gives a similar result.

To characterize the phase noise of MLLs, a single sideband power spectra density (SSB-PSD) of its phase noise, $S_{\phi}(f)$, is commonly used. $S_{\phi}(f)$ gives the information of how different noise frequencies (f) contribute to the overall phase noise. It can be calculated from the RF spectra and is defined as the RF power in a 1 Hz bandwidth at different offset frequencies (f) with respect to the RF power at the carrier frequency (f_c , the fundamental repetition frequency in this work).

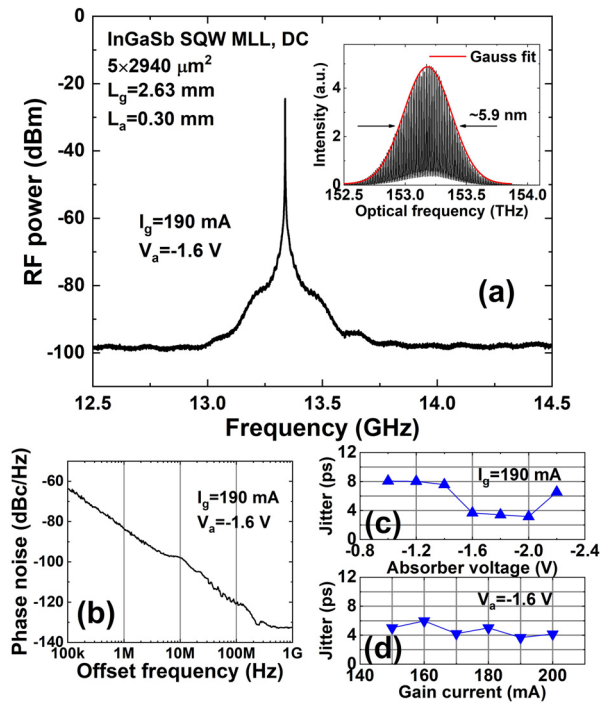


FIG. 2. (a) A typical RF spectrum at 20 $^{\circ}\text{C}$ ($I_g = 190$ mA, $V_a = -1.6$ V) of the tested two-section MLL. The inset shows the corresponding optical spectrum under this bias condition. (b) SSB-PN spectrum of the RF signal in (a) in the 100 kHz to 1 GHz range. (c) V_a -dependent integrated jitter at $I_g = 190$ mA. (d) I_g -dependent integrated jitter at $V_a = -1.6$ V.

Once we have $S_{\phi}(f)$, the integrated timing jitter (σ_j) can be calculated and used as a straightforward measure of the phase noise. It can be expressed using the popular von der Linde method²⁰

$$\sigma_j^2 = \frac{1}{2\pi f_c} \sqrt{2 \int_{f_1}^{f_2} S_{\phi}(f) df}, \quad (1)$$

where f_1 and f_2 determine the offset frequency range over which the power spectral density is integrated. In this work, we use 100 kHz and 1 GHz as the integration borders.

Figure 2(b) shows the SSB-PN spectrum of the RF signal in Fig. 2(a) in the 100 kHz–1 GHz range. The integrated jitter under this bias condition ($I_g = 190$ mA, $V_a = -1.6$ V) is calculated to be ~ 3.67 ps. Actually, when applying any I_g which is well beyond the lasing threshold (within a reasonable range), there exists a suitable range of V_a to achieve stable mode locking. When V_a is less negative than this range, the mode locking operation will be with a large continuous wave (cw) component, while when V_a exceeds the range, Q-switching instability will emerge.²¹ For example, at $I_g = 190$ mA as in Figs. 2(a) and 2(b), stable mode locking can be achieved with V_a ranging from -1 V to -2.2 V. The integrated jitter within this V_a range is shown in Fig. 2(c). This variation trend of the integrated jitter is typical for the tested laser. To be specific, for a given I_g , there is no monotonous dependence of the integrated jitter on V_a . It needs the coordination between I_g and V_a to reach the optimal jitter. Likewise, the jitter dependence on I_g when $V_a = -1.6$ V is also shown in Fig. 2(d). This finding also applies at high temperatures and is similar to that reported in Refs. 9 and 10.

Next, we will be focusing on the more important temperature dependence of the phase noise properties. Stable mode locking was achieved up to 60°C , and when temperature rises, it can be maintained at a less negative V_a (starting from -1 , -0.8 , and -0.4 V at 20, 40, and 60°C , respectively). This is mainly attributed to the enhanced thermal sweep-out of the carriers at elevated temperatures.^{22,23}

Figure 3(a) shows three typical RF spectra at 20, 40, and 60°C . According to the figure, the RF signal narrows consistently and significantly with temperature, while its power drops gradually. In addition to the typical spectra, RF spectra corresponding to the lowest jitters at these three temperatures are also shown in Fig. 3(b), and the same variation trend is seen. It is known that RF signal narrowing means phase noise improvement. This is clearly demonstrated in Fig. 3(c) which displays the SSB-PN spectra corresponding to the spectra in Fig. 3(b) (minimum integrated jitters at 20, 40, and 60°C , respectively). The integrated jitter reduces from 3.15 ps at 20°C all the way down to 1.39 ps at 60°C . The offset frequency to hit the thermal noise floor decreases dramatically from 400 MHz at 20°C to 4 MHz at 60°C , and the phase noise at 60°C remains being lower before the thermal noise floor.

We consider that this phase noise properties' improvement is mainly due to reduced amplified spontaneous emission (ASE) noise at higher temperatures. Figure 4 shows the optical spectra corresponding to the lowest jitters at different temperatures [same bias conditions as those in Fig. 3(b)]. One useful parameter that can be extracted from the spectra is the peak-to-valley ratio of the involved laser modes. To show this parameter more clearly, the spectra are displayed in the dB scale. The peak-to-valley ratio of the laser modes at around the highest power keeps increasing from ~ 11.2 dB at 20°C to ~ 12.6 dB at 60°C , indicating that the ASE noise power drops at higher temperatures.²⁴ Another information given by this figure is an obvious wavelength redshift with temperature which is due to bandgap shrinkage.

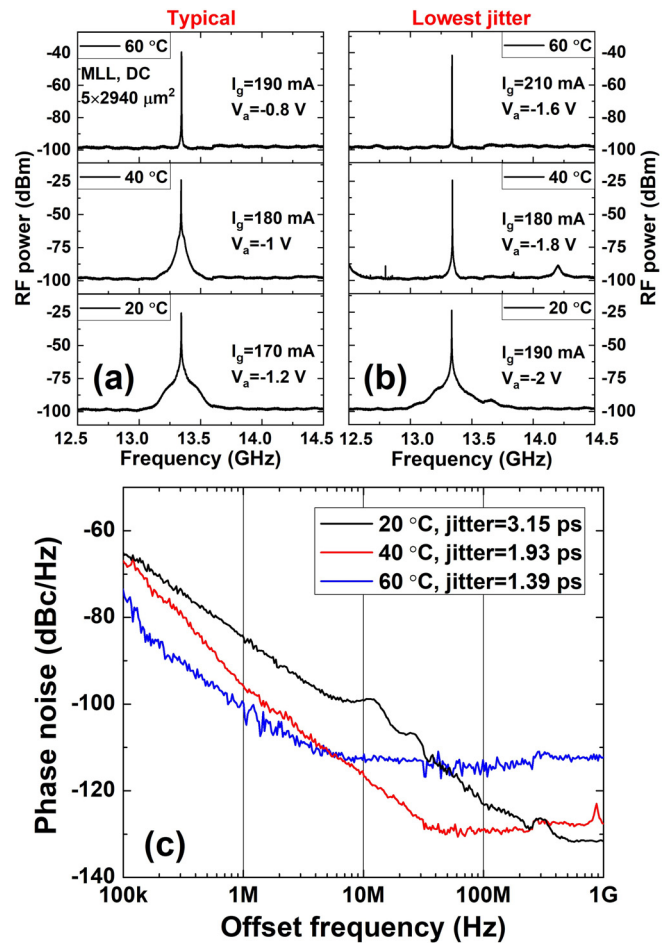


FIG. 3. (a) Three typical RF spectra at 20, 40, and 60°C of the tested two-section MLL. (b) RF spectra corresponding to the lowest jitters at these three temperatures. (c) SSB-PN spectra corresponding to the spectra in (b) (minimum integrated jitters at 20, 40, and 60°C , respectively).

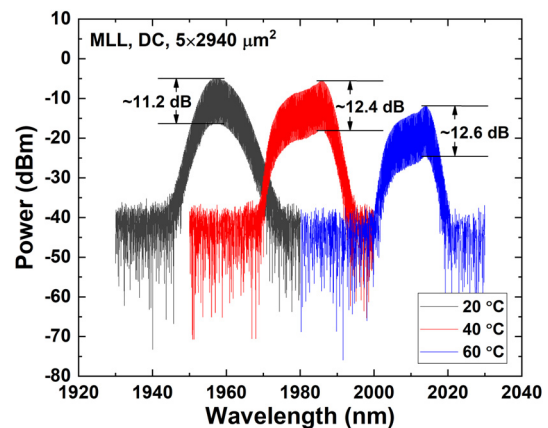


FIG. 4. Optical spectra corresponding to the lowest jitters at different temperatures of the tested two-section MLL [same bias conditions as those in Fig. 3(b)].

In addition to the three spectra in Fig. 4, for all the measured optical spectra, the overall ASE noise reduces noticeably with temperature. Although this will not cause the jitters at higher temperatures to be lower under all bias conditions because jitter is also determined by the mode locking condition, a weakening in the ASE noise power will anyway be favorable to lower the overall jitter and push the lowest achievable value further.

Another thing worth mentioning are the corresponding light output powers for the three cases in Fig. 3(c) which are 6.1, 3.5, and 2.3 mW at 20, 40, and 60 °C, respectively. Therefore, a trade-off between output power and low-noise operation may commonly exist due to the inevitable power drop as temperature rises.

In conclusion, the bias- and temperature-dependent phase noise properties (expressed as SSB-PSD and integrated jitter) of a two-section GaSb-based passively mode-locked laser are systematically investigated. At a fixed temperature, there is no monotonous dependence of phase noise on the bias condition. It needs the coordination between the gain current and the absorber voltage to reach the optimal jitter. More important, the phase noise properties improve obviously at elevated temperatures with the minimum integrated jitter reducing obviously from 3.15 ps at 20 °C to 1.39 ps at 60 °C (100 kHz–1 GHz). We consider that the primary cause is the reduced ASE noise confirmed by the extracted peak-to-valley ratio of the involved laser modes. We believe that this study provides an important insight into the carrier behaviors and noise performance of mode-locked semiconductor lasers at high temperatures, which is meaningful for them to better meet the requirements in many practical applications.

This work was supported in part by the National Research Foundation of Singapore (No. NRF-CRP12-2013-04), the National Natural Science Foundation of China (Nos. 61964007 and 61790582), and the Key-Area Research and Development Program of Guangdong Province (No. 2020B0303020001).

DATA AVAILABILITY

The data that support the findings of this study are available from the corresponding author upon reasonable request.

REFERENCES

¹E. Rafailov, M. Cataluna, and W. Sibbett, *Nat. Photonics* **1**, 395 (2007).

- ²M. G. Thompson, A. R. Rae, M. Xia, R. V. Pentyl, and I. H. White, *IEEE J. Sel. Top. Quantum Electron.* **15**, 661 (2009).
- ³M. Kuntz, G. Fiol, M. Laemmlin, C. Meuer, and D. Bimberg, *Proc. IEEE* **95**, 1767 (2007).
- ⁴K. Merghem, R. Teissier, G. Aubin, A. M. Monakhov, A. Ramdane, and A. N. Baranov, *Appl. Phys. Lett.* **107**, 111109 (2015).
- ⁵T. Feng, L. Shterengas, T. Hosoda, A. Belyanin, and G. Kipshidze, *ACS Photonics* **5**, 4978 (2018).
- ⁶K. Holc, T. Weig, W. Pletschen, K. Köhler, J. Wagner, and U. T. Schwarz, *Proc. SPIE* **8625**, 862515 (2013).
- ⁷J. N. Kemal, P. Marin-Palomo, V. Panapakkam, P. Trocha, S. Wolf, K. Merghem, F. Lelarge, A. Ramdane, S. Randel, W. Freude, and C. Koos, *Opt. Express* **27**, 31164 (2019).
- ⁸A. R. Rae, M. G. Thompson, R. V. Pentyl, I. H. White, A. R. Kovsh, S. S. Mikhlin, D. A. Livshits, and I. L. Krestnikov, *Proc. SPIE* **6184**, 61841F (2006).
- ⁹M. T. Todaro, J.-P. Tourrenc, S. P. Hegarty, C. Kelleher, B. Corbett, G. Huyet, and J. G. McInerney, *Opt. Lett.* **31**, 3107 (2006).
- ¹⁰F. Kéfélian, S. O'Donoghue, M. T. Todaro, J. G. McInerney, and G. Huyet, *IEEE Photonics Technol. Lett.* **20**, 1405 (2008).
- ¹¹K. Merghem, A. Akrouf, A. Martinez, G. Moreau, J.-P. Tourrenc, F. Lelarge, F. Van Dijk, G.-H. Duan, G. Aubin, and A. Ramdane, *Opt. Express* **16**, 10675 (2008).
- ¹²K. Scholle, S. Lamrini, P. Koopmann, and P. Fuhrberg, in *Frontiers in Guided Wave Optics and Optoelectronics*, edited by B. Pal (InTech, Rijeka, 2010), Chap. 21.
- ¹³J. Geng and S. Jiang, *Opt. Photonics News* **25**, 34 (2014).
- ¹⁴A. Schliesser, N. Picqué, and T. W. Hänsch, *Nat. Photonics* **6**, 440 (2012).
- ¹⁵S. Shu, G. Hou, J. Feng, L. Wang, S. Tian, C. Tong, and L. Wang, *Opto-Electron. Adv.* **1**, 170003 (2018).
- ¹⁶X. Li, H. Wang, Z. Qiao, X. Guo, G. I. Ng, Y. Zhang, Z. Niu, C. Tong, and C. Liu, *Appl. Phys. Lett.* **111**, 251105 (2017).
- ¹⁷H. Liu, T. Kamiya, and B. Du, *IEEE J. Quantum Electron.* **22**, 1579 (1986).
- ¹⁸M. A. Cataluna, E. U. Rafailov, A. D. McRobbie, W. Sibbett, D. A. Livshits, and A. R. Kovsh, *IEEE Photonics Technol. Lett.* **18**, 1500 (2006).
- ¹⁹X. Huang, A. Stintz, H. Li, A. Rice, G. T. Liu, L. F. Lester, J. Cheng, and K. J. Malloy, *IEEE J. Quantum Electron.* **37**, 414 (2001).
- ²⁰D. von der Linde, *Appl. Phys. B* **39**, 201 (1986).
- ²¹X. Li, H. Wang, Z. Qiao, X. Guo, W. Wang, G. I. Ng, Y. Zhang, Y. Xu, Z. Niu, C. Tong, and C. Liu, *Opt. Express* **26**, 8289 (2018).
- ²²M. A. Cataluna, E. A. Viktorov, P. Mandel, W. Sibbett, D. A. Livshits, J. Weimert, A. R. Kovsh, and E. U. Rafailov, *Appl. Phys. Lett.* **90**, 101102 (2007).
- ²³M. A. Cataluna, D. B. Malins, A. Gomez-Iglesias, W. Sibbett, A. Miller, and E. U. Rafailov, *Appl. Phys. Lett.* **97**, 121110 (2010).
- ²⁴S. Srinivasan, E. Norberg, T. Komljenovic, M. Davenport, G. Fish, and J. E. Bowers, *IEEE J. Sel. Top. Quantum Electron.* **21**, 24 (2015).